

AUTOMATED DELAY MEASUREMENT SYSTEM FOR AN EARTH STATION FOR TWO-WAY SATELLITE TIME AND FREQUENCY TRANSFER

Gerrit de Jong and Michel C. Polderman
NMI Van Swinden Laboratorium
P.O. Box 654
2600 AR DELFT
The Netherlands

Abstract

The measurement of the difference of the transmit and receive delays of the signals in a Two-Way Satellite Time and Frequency Transfer (TWSTFT) earth station is crucial for its nanosecond time transfer capability. Also, the monitoring of the change of this delay difference with time, temperature, humidity, or barometric pressure is important for improving the TWSTFT capabilities.

An automated system for this purpose has been developed from the initial design at NMI-VSL. It calibrates separately the transmit and receive delays in cables, amplifiers, upconverters, and downconverters, and antenna feeds. The obtained results can be applied as corrections to the TWSTFT measurement, when, before and after a measurement session, a calibration session is performed. Preliminary results obtained at NMI-VSL will be shown. Also, if available, the results of a manual version of the system that is planned to be circulated in September 1994 together with a USNO portable station on a calibration trip to European TWSTFT earth stations.

1. Introduction

The Two-Way Satellite Time and Frequency Transfer (TWSTFT) method (Fig. 1) is used to compare two clocks or time scales which are often located at great distances from each other. The time scale events, normally the 1 pulse per second (1pps) signals, are simultaneously transmitted to the other clock by means of a transmission link through a satellite, normally a geostationary communication satellite. The delays in troposphere, ionosphere, satellite transponder and earth station equipment cancel in first order, the Sagnac correction can be calculated. The biggest source of asymmetry error is the sum of the transmit and receive equipment delay differences of the earth stations involved. For absolute time scale difference determination this sum has to be calibrated to the required uncertainty.

One method to accomplish this is to co-locate the two earth stations and do TWSTFT using a common clock.

If this is not feasible, a third earth station is subsequent co-located with both stations, and the relative delay difference of each of the two stations is calculated.

A third method is the separate measurement (calibration) at each earth station of the absolute transmit delay and the receive delay by using a special modified translator or Satellite Simulator in front of the antenna and some additional equipment. The required sum of the differences can then be calculated. This method was first described by De Jong (1989).

This paper addresses further progress. The method is developed by simplifying and enhancing the Simulator, a transportable equipment set has been constructed and finally an automated calibration method has been developed and realized.

2. Calibration principle with satellite simulator.

2.1 Single frequency down converting satellite simulator

The transmit frequency F_{up} of a earth station to a communication satellite (Fig. 2) for Ku-band is typical 14 GHz, the receive frequency F_{dn} is lower by a fixed amount, the translation frequency DF. This DF is for e.g. Intelsat in the USA 2295 MHz, in Europe 1495 MHz.

A double balanced mixer suitable for these frequency bands can be used for down conversion by feeding the translation frequency DF into the IF-port (Fig. 3a). When the transmit signal is fed into the RF-port then the LO-port contains the frequency difference ($F_{up} - DF$), which is the receive frequency F_{dn} . The required power level for DF at the IF-port is 3 to 7 dBm. The conversion loss between the input signal at the RF-port and the output signal at the LO-port is normally less than 10 dB.

An antenna connected to the RF-port receives the transmitted signal in one polarisation and a similar antenna, but with orthogonal polarisation, at the LO-port sends the down converted signal back to the main antenna as receive signal. So this device simulates to what a satellite transponder does, but now the distance to the antenna is short and known.

When performing TWSTFT using this Satellite Simulator, in this case receiving the own signal back (ranging) (Fig. 4), the round-trip delay is measured from modem through cables, the up-converter, the power amplifier, the antenna feed, the distance to the satellite simulator (twice), the internal delay of the simulator, and the complete receive equipment path. The continued measurement of this sum delay already gives an impression of the instability of the equipment, but what we need is the difference between transmit and receive chain. The next chapter is a further step towards this.

2.2 Calibration with a dual frequency dual mixer simulator.

The translation frequency DF can be obtained from a second mixer providing DF as the sum frequency of two other frequencies (Fig. 3b). For a reason we will see later, one of these frequencies is chosen to be equal to the 70 MHz IF frequency of the used modem. So the second frequency should be (DF-70) MHz. However, the output level of the second mixer is too low to excite the first mixer, and a wide band amplifier needs power, is active, and has a

delay to be measured. A solution is to place the RF and LO ports of the two mixers, as two down converters, in series (Fig. 3c).

This works similar to the circuit (Fig. 4) of paragraph 2.1 (see Fig. 5): the transmitted signal is received back from the simulator, provided that 70 MHz and (DF-70) MHz signals of >3 dBm are fed into the IF-ports of the two mixers. The sum DLY1 of the transmit and receive delays $TT(k)+TR(k)$ can be measured.

The 70 MHz Continuous Wave (CW) signal and the 70 MHz Transmit PN modulated signal from the modem are then interchanged (Fig. 6). The 70 MHz CW signal is up-converted to the transmit frequency F_{up} . The input to the mixers has become a unmodulated CW signal of e.g. 14 GHz. But the down conversion now uses a 70 MHz PN modulated signal, so the output signal from the satellite simulator is a PN modulated signal as before. Now the sum (DLY2) of the 70 MHz Reference Cable from modem TX output to the 70 MHz input of the simulator and the receive chain delay $TR(k)$ is measured.

By using two other cables the delay of the used 70 MHz Reference Cable (DLY3) can be calibrated. Subtraction of DLY3 from DLY2 gives the receive delay $TR(k)$. Subtraction of $TR(k)$ from DLY1 gives the transmit delay $TT(k)$. If this procedure is followed at both earth stations, and the values exchanged, the needed sum of transmit and receive delay differences can be calculated; the internal modem transmit delay should also be measured using a digital oscilloscope or the method described by De Jong (1989) and the resulting internal delay difference should be incorporated in $TT(k)$ and $TR(k)$.

3. Improvement: dual frequency single mixer simulator

The simulator with two mixers in series works well. However, there are some disadvantages. Firstly the asymmetry: the mixer with the 70 MHz port is closer to one of the antennas, giving a small delay difference. Secondly, the 70 MHz signal is connected directly to the mixer IF-port which can give mismatch and consequently signal reflections leading to a "multi-path" effect. Thirdly the total conversion loss is doubled: 15 – 20 dB. Realizing that a mixer has its properties due to its non-linear characteristic, it was realized that a linear addition of two signals fed into a non-linear device should produce spectral components at the sum frequency as well as the difference frequency.

For addition of the 70 MHz and the (DF-70) MHz signals we have used a wide band (DC-12 GHz) resistive power combiner PD (Fig. 7). This device has 3 ports with equal properties and delay to the other ports. One disadvantage is the 6 dB insertion loss but the mismatch of the mixer IF-port to the cable is also reduced by this decoupling. Good results were obtained. The 70 MHz signal level for both the CW and the PN modulated signal should be at least at +8 dBm before the power combiner. An amplifier is added in the 70 MHz CW path for this purpose.

3.2 Construction of the Satellite Simulator

The resistive power combiner is placed in the satellite simulator box together with the mixer and the two antennas (Fig. 8). As inexpensive antennas we use two wave guide to coax adapters. They work fine, but might give some reflection back to the antenna dish.

The plastic material of the box is transparent to the frequencies concerned, so no hole was needed for the antennas. A nice symmetric component lay-out was adopted. Interconnections have been made (thanks to Mr. A. Trarbach, NMI Electronics Lab!) with semi-rigid coaxial cable and SMA connectors. The internal delay from antenna to antenna is 2 ns and matches the delay from the 70 MHz input to both antennas within 0.1 ns.

4. Portable Satellite Simulator Calibration equipment.

Two Satellite Simulators were built accordingly. One was placed in front of our fixed TWSTFT earth station. The other was used to assemble a portable earth station delay calibrator. This was used at several stations during the European TWSTFT Calibration Trip with the USNO movable earth station (FAST) in September and October 1994; it was also used to calibrate the FAST delays. The equipment was completed with two boxes (see Fig. 5), one containing a 5 MHz distribution amplifier and a 70 MHz source, both derived from the 5 or 10 MHz reference at the station and the other containing the 70 MHz amplifier and a source for (DF-70) MHz, which is 1425 MHz for Europe. This frequency was also phase locked to the 5 MHz reference at the stations. It is tunable in 5 MHz steps. When using the same translation frequency as in the satellite, the signal from the satellite is also present during calibration. To avoid possible interference, the antenna pointing should be changed to avoid pointing to the satellite or the source should be tuned to a slightly different translation frequency. Most stations have mechanical adjustment for azimuth and elevation, therefore the source was tuned to 1430 MHz. The receive frequency for the calibration was now 5 MHz lower than for the satellite. This is expected not to give a significant delay difference. Also a set of cables, up to 100 m length was included as well as the power supplies. The total mass was about 30 kg.

5. Automation of the Calibration

From TWSTFT experiments it is seen that at integration times greater than 200–300 s the Allan Deviation indicates an increase in instability. One of the reasons can be the change of the delays in the station equipment. Only if the delays in the transmit and in the receive equipment changes by the same amount at the same time, they cancel and do not influence the instability. The proposed method with the Satellite Simulator measures the TX and RX delays separately. So this method can be used for investigation of the delay changes but also to measure and then correct the data for possible changes. In the latter case the long term frequency transfer capability of TWSTFT would also improve. To do this, the calibration has to be automated.

NMI VSL has developed a automated measurement system for all equipment and cables. However, with exception of the internal 70 MHz TX and RX modem delays; this modem is in

a temperature and humidity controlled room and are expected to have the least change.

5.1 Design considerations

The automation should not disturb the correct termination of cables. When a cable carrying a signal temporarily is not used, it is to be terminated correctly. A solution for this is the use of so-called transfer switches: when a switch is activated the existing path is changed and a second path is substituted (Fig. 9). These switches are available in the form of coil-activated coaxial switches, relays. These relays are activated from a IEEE-488 bus through a relay adapter.

Our MITREX 2500 was already made programmable through such a device, and the same applies to the setting of the transmit frequency and the receive frequency. The calibration of the total delay of the 70 MHz reference path (the 70 MHz CW cable, the amplifier, and even the 70 MHz cable to the Satellite Simulator) is also included (Fig. 10).

5.2 Description of the measurements (Fig. 10).

5.2.1. Measurement of the sum of internal TX and RX modem delays.

Switch the modem into the TESTLOOP Mode. Now the TX output and the RX input of the modem are interconnected internally. The average Time Interval Counter (TIC) reading is stored as [1].

5.2.2 Measurement of the 70 MHz Reference path.

5.2.2.1 Determination of sum of the delay of the 70 MHz TX and the 70 MHz RX cable.

Only the switches A and B are activated. Two ports of the power combiner PC are used to interconnect the far ends of the TX and RX cables, the third port is terminated in a termination T. The TIC reading is averaged and stored as [4].

subsubsubsect5.2.2.2 Determination of sum of the delay of the 70 MHz CW + amplifier and the 70 MHz TX cable.

Only switches 1, 2, 3, C and A are activated. Two ports of the Power Combiner (PC) are used to interconnect the far ends of the CW and RX cables, the third port is terminated in a termination T. The TIC reading is stored as [5].

5.2.2.3 Determination of sum of the delay of the 70 MHz CW + amplifier and the 70 MHz RX cable.

Only the switches 1, 3, C and B are activated. Two ports of the power combiner PC are used to interconnect the far ends of the CW and RX cables, the third port being terminated in a termination T. The TIC reading is stored as [6].

5.2.2.4 Determination of sum of the delay of the 70 MHz CW + amplifier, the two cables to the Satellite Simulator and the 70 MHz RX cable.

Only the switches 1, D and B are activated. Two ports of the power combiner PC are used to interconnect the far end of the CW cable, the two Satellite Simulator cables and RX cables, the third port is terminated in a termination T. The two cables to the Satellite Simulator are

interconnected by a power combiner in the Satellite Simulator. The TIC reading is stored as [7].

5.2.2.5 Calculation of the 70 MHz Reference path delay.

The delay of the 70 MHz CW cable + amplifier is: $0.5([5] - [1]) + ([6] - [1]) - ([4] - [1])$ [8]
The delay of the sum of the two cables to the Satellite Simulator is $[7] - [6]$; because of the fact that the two cables are co-located and of the same type the delay of one cable is calculated by the ratio R of the length of that cable compared to the sum of the lengths of both cables. In our case both cables have the same length, so $R = 0.5$, thus the delay [9] of one cable is: $0.5([7] - [6])$.

The total 70 MHz Reference path [10] is now: $[8] + [9]$

5.2.2. Measurement of the sum of all TX and RX delays.

For this measurement all relays remain in the inactive position. However, the receive frequency is lowered by 5 MHz to receive the signal from the Simulator in stead of the signal from the satellite (otherwise the antenna should be pointed away from any satellite). The reading of the TIC is averaged and stored as [2].

5.2.3. Measurement of the sum of 70 MHz reference cable and the RX delays.

Now only switch 1 is activated, so the 70 MHz CW and the 70 MHz TX signals are interchanged. The average TIC reading is registered as [3].

5.2.4 Calculation of the TX and RX delays.

The RX delay is: $([3] - [1]) - [10]$ [11] The TX delay is: $([2] - [1]) - [11]$ [12]

5.3 Wiring Delays

In the calculations in 4.2 the small and constant delays in the relays, power combiners and associated sort wirings were not mentioned, but these small delays of up to 1 ns were measured and are used as correction constants in the software. It appears that the length of a signal path through a high frequency device mostly is a good measure for its delay, the same as for coaxial cable: 5 ps for 1 millimeter.

6. Advantages of incorporation of Calibration sessions in regular TWSTFT measurements.

The Calibration measurements as described in 4.2 can be performed in a calibration session. Such a session can precede and follow a TWSTFT session. From the delay change, a rate of change can be determined and the results from the TWSTFT sessions can then be corrected for that change.

Changes in cables and equipment are also detected and can be corrected for. Corrections could be done also during a long period; when both of a pair of TWSTFT stations do this,

then also the frequency transfer instability of the TWSTFT between them is improved because of a lower flicker floor. The remaining instrumentation instability source will then be restricted to the instability of the modems and the counters, apart from the reference clocks themselves.

7. Status and some results at NMI-VSL

Part of the system was installed and used since July 1994; the Relay system is now also installed (nov. '94), except the connections of the relays to the relay interface. Changes to our software will then be performed to incorporate the fully automated calibration in a Calibration session.

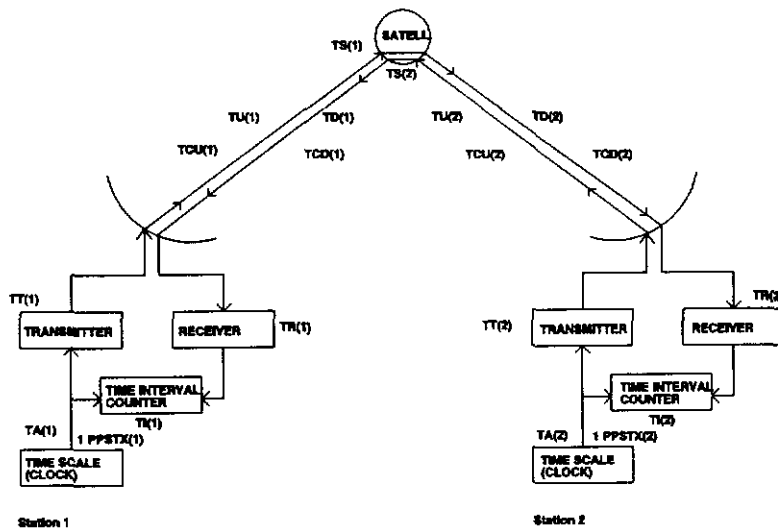
Fig. 11 shows the behaviour over about 4 months of our modem when TESTLOOP measurements are done. Fig. 12 shows results over the same period of Satellite Simulator loop (TX + RX delay) measurements. Results for the automated calibration system will become available next year. Also results from calibrations with the portable delay calibrator compared to the FAST calibration will be reported later.

8. Conclusion

The feasibility of this fully automated delay calibration system for a TWSTFT earth station using a special modified Satellite Simulator has been shown. It clearly detects and measures delay changes in the TX and RX path separately. It is a suitable and cost-effective tool to improve the instability of frequency and time transfer by means of the TWSTFT method.

9. References

- Jong, G de 1989, "Accurate Delay Calibration for Two-Way Time Transfer Earth Stations", Proc. 21th PTTI Meeting, Redondo Beach, pp. 107-115.
- Jong, G de 1993, "Two-Way Satellite Time Transfer: Overview and recent developments", Proc. 25th PTTI Meeting, Marina Del Rey CA, NASA Conf. Publication 3267, pp. 101-117
- Veenstra, L B 1990, "International Two-Way Satellite Time Transfer using INTEL-SAT space segment and small earth stations", Proc. 22nd PTTI Meeting, pp. 393-400.
- Kirchner, D 1991, "Two-Way Time Transfer Via Communication Satellites", Proceedings of the IEEE, Vol.79, No. 7, pp. 983-990.
- Davis, J A and Pearce, P R 1993, "Characterization of the signal delays in a ground station designed for satellite two way time transfer", Proc. EFTF 93, Neuchatel, pp. 113-118.



The timescale difference is given by:

$$\begin{aligned}
 TA(1) - TA(2) = & +0.5\{TI(1)\} && \text{(TIC reading at 1)} \\
 & -0.5\{TI(2)\} && \text{(TIC reading at 2)} \\
 & +0.5\{TS(1) - TS(2)\} && \text{(Satellite delay difference)} \\
 & +0.5\{TU(1) - TD(1)\} && \text{(Up/down difference at 1)} \\
 & -0.5\{TU(2) - TD(2)\} && \text{(Up/down difference at 2)} \\
 & +0.5\{TT(1) - TR(1)\} && \text{(TX/RX difference at 1)} \\
 & -0.5\{TT(2) - TR(2)\} && \text{(TX/RX difference at 2)} \\
 & -0.5\{TCD(1) - TCU(1)\} && \text{(Sagnac + sat. movement)} \\
 & +0.5\{TCD(2) - TCU(2)\} && \text{(Sagnac + sat. movement)}
 \end{aligned}$$

Figure 1. Two-Way Satellite Time and Frequency Transfer Method

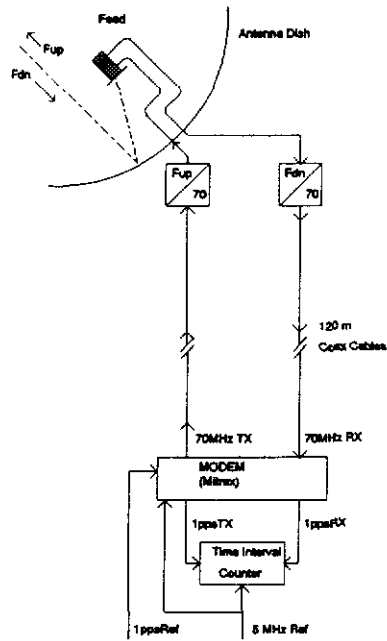


Figure 2. Typical TWSTFT Earth Station Configurati

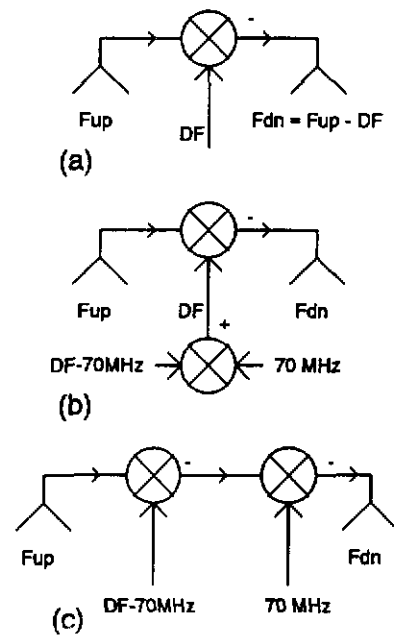


Figure 3. Different Translator Mixer Schemes

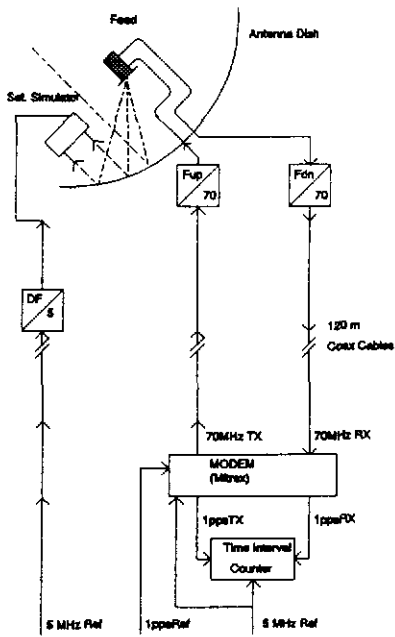


Figure 4. Ranging Using a Satellite Simulator

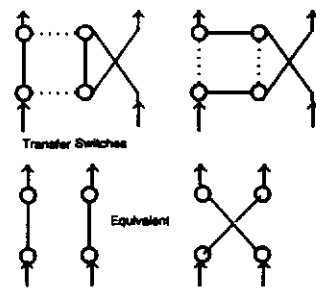


Figure 9. Transfer Switches

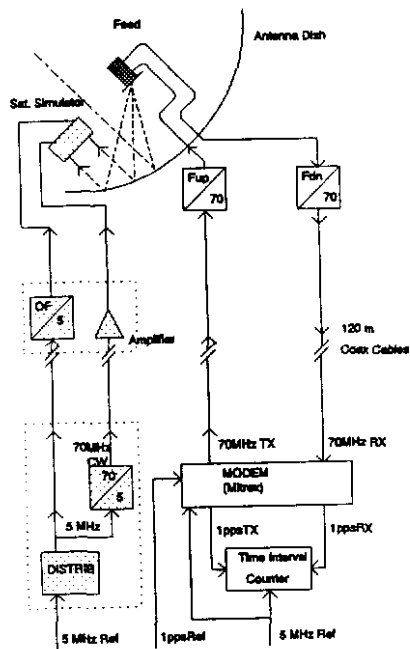


Figure 5. (Portable) Satellite Simulator for Measuring $TR(k) + TT(k)$

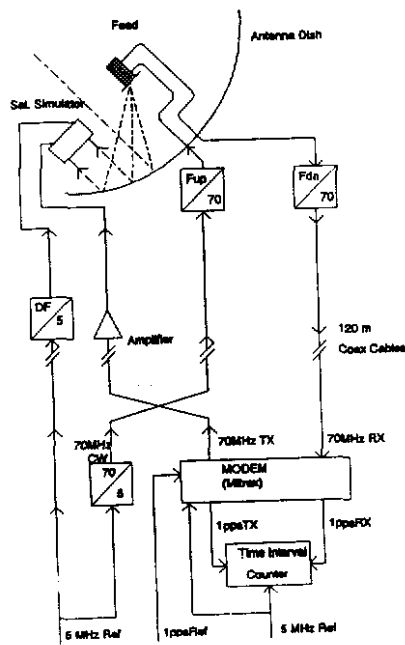


Figure 6. Satellite Simulator for Measuring $TR(k) + Reference Path$

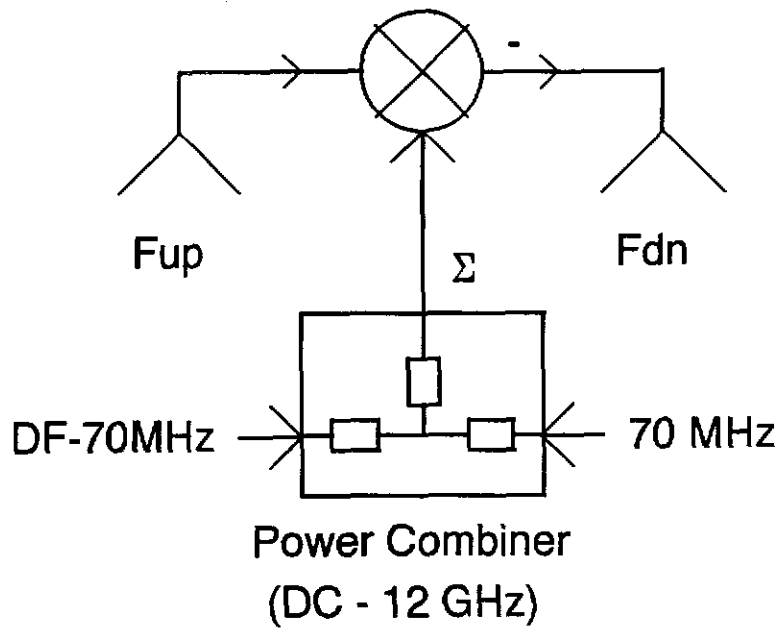


Figure 7. Use of Power Combiner and One Mixer

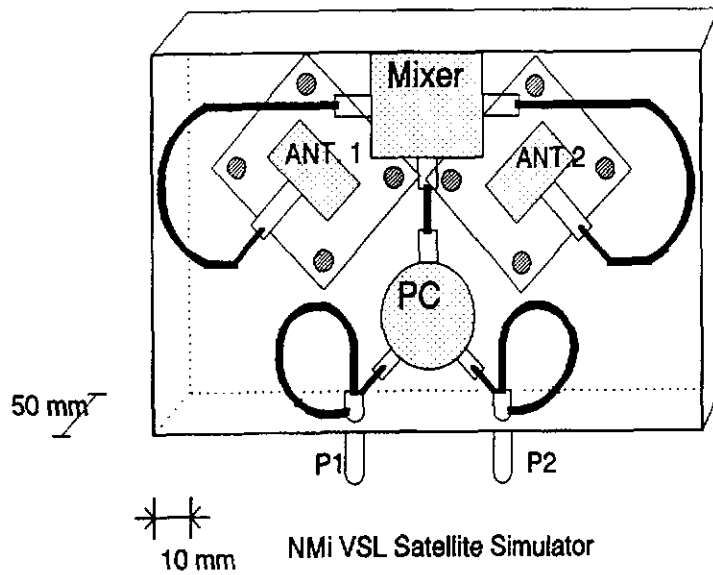


Figure 8. Layout of the NMi Satellite Simulator

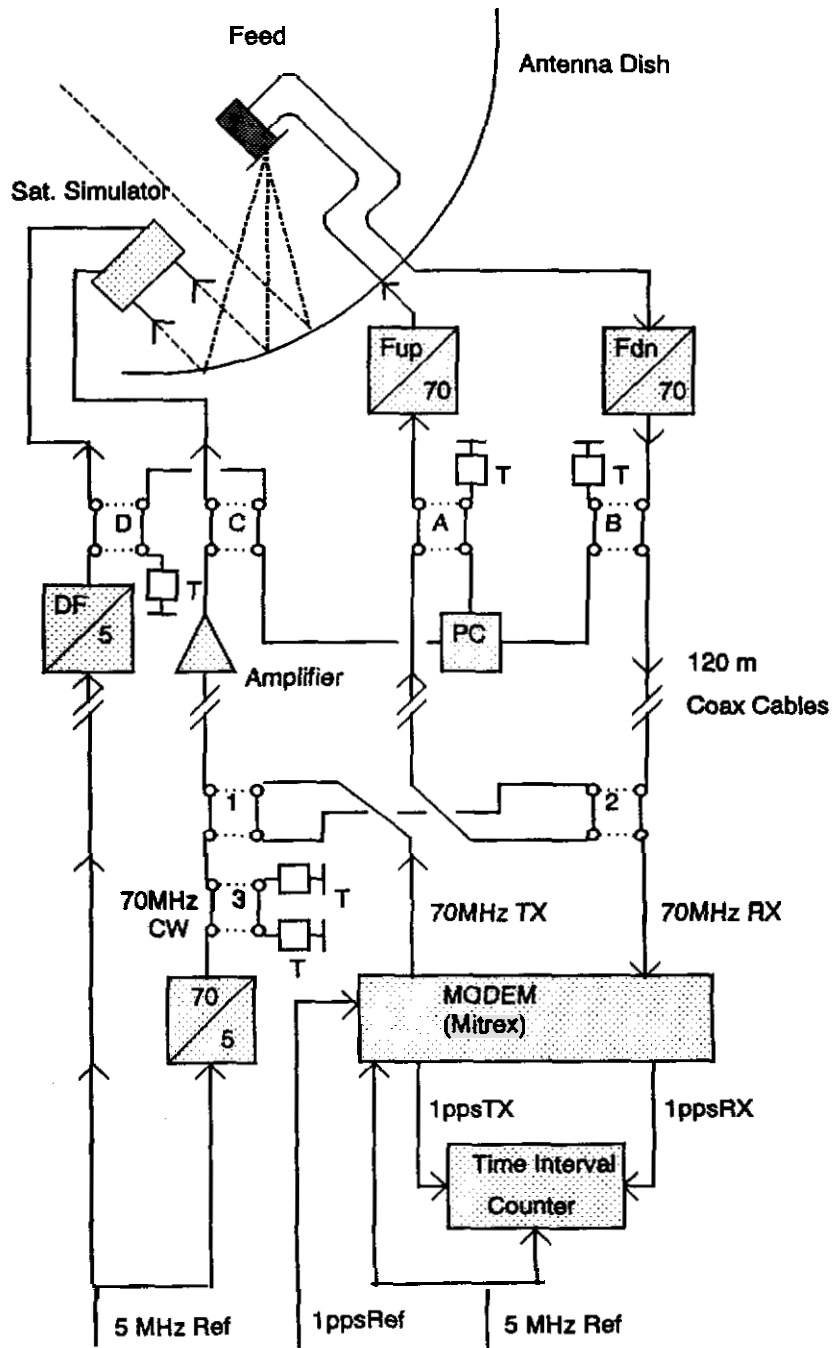


Figure 10. Automatic Delay Calibration System for TWSTFT Stations

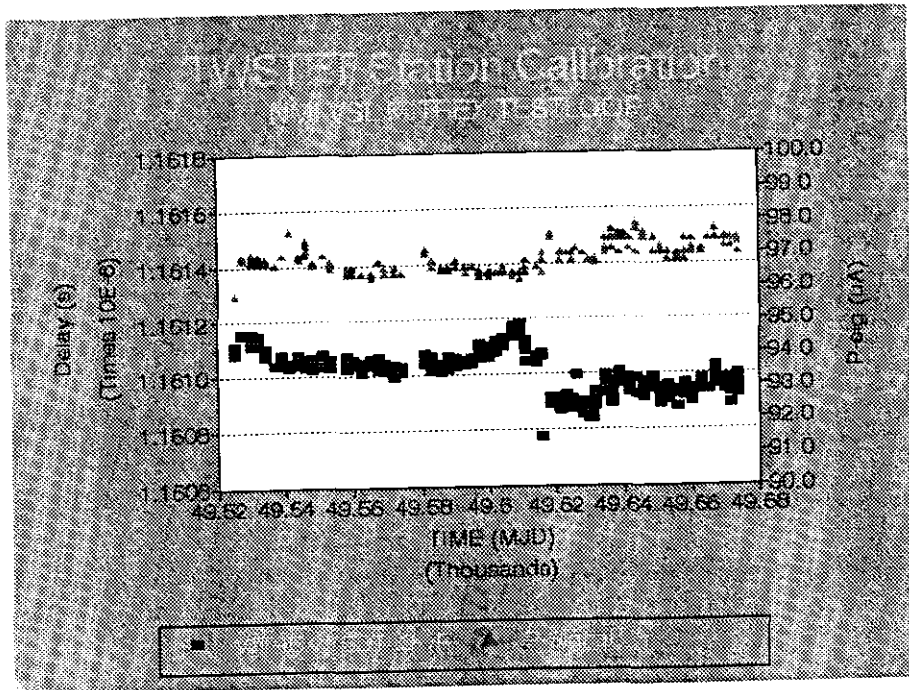


Figure 11. VSL MITREX Modem TESTLOOP Delay July - November 1994

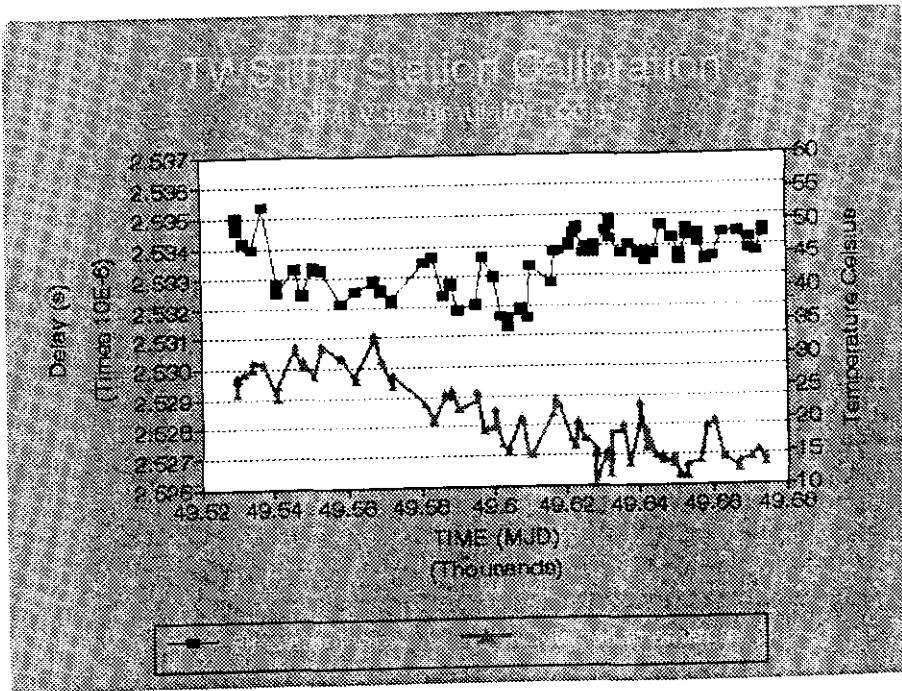


Figure 12. VSL RX+TX Delay July - November 1994



STUDY OF TROPOSPHERIC CORRECTION FOR INTERCONTINENTAL GPS COMMON-VIEW TIME TRANSFER

W. Lewandowski
Bureau International des Poids et Mesures
Pavillon de Breteuil
92312 Sèvres Cedex, France

W.J. Klepczynski, M. Miranian
United States Naval Observatory
Washington, DC 20392-5420, USA

P. Grüdler, F. Baumont
Observatoire de la Côte d'Azur
Av. Copernic, 06130 Grasse, France

M. Imae
Communications Research Laboratory
Nukui Kita-machi, Koganei-shi, 184 Tokyo, Japan

Abstract

Current practice is to incorporate general empirical models of the troposphere, which depend only on the station height and the elevation of the satellite, in GPS time receivers used for common-view time transfer. Comparisons of these models with a semi-empirical model based on weather measurements show differences of several nanoseconds. This paper reports on a study of tropospheric correction during GPS common-view time transfer over a short baseline of about 700 km, and three long baselines of 6400 km, 9000 km and 9600 km. It is shown that the use of a general empirical model of the troposphere within a region where the climate is similar does not affect time transfer by more than a few hundreds of picoseconds. For the long distance links, differences between the use of general empirical model and the use of a semi-empirical model reach several nanoseconds.

INTRODUCTION

Among the improvements open to GPS common-view time transfer is increased accuracy in the estimation of the tropospheric delay. It has been assumed until recently that, for satellite elevations above 30°, a general empirical model, depending only on the station height and

satellite elevation, is sufficient. However, when carrying out common-view time transfer over long distances (9000 km), elevations as low as 20 are unavoidable. Also, different types of receivers use different tropospheric models which can differ by a few nanoseconds for angles of low elevation^[1, 2]. Progress can be made by implementing recently established standards for receiver software which include a common model for estimating signal delays arising from tropospheric refraction^[3].

Recent comparisons of the models currently used by GPS time receivers with a semi-empirical model based on weather measurements show differences of several nanoseconds^[4, 5, 6]. This discrepancy increases for observations performed in hot and humid regions of the world.

This paper reports on comparisons of GPS common-view time transfers performed using the tropospheric models incorporated in the receivers with transfers performed using a semi-empirical model. These comparisons have been carried out for one short baseline of about 700 km, and three long baselines of about 6400 km, 9000 km and 9600 km. It is shown that the use of the general empirical model of the troposphere within a region of similar climate does not affect time transfer by more than a few hundreds of picoseconds, while for the intercontinental GPS time links, differences between the general empirical model and a semi-empirical model reach several nanoseconds.

TROPOSPHERIC DELAY AND ITS MODELS

The troposphere is the lower layer of the atmosphere extending from ground level to the base of the ionosphere. For radio frequencies, delay due to the troposphere ranges typically from about 10 ns for the zenith to about 100 ns for an elevation of 5° : it depends on the thickness of the troposphere and the content of water vapour along the line of sight. Tropospheric delay is commonly expressed as the sum of two components 'dry' and 'wet'. The 'wet' component is due to water vapour and can reach 15 % of the total correction.

At radio frequencies, unlike optical frequencies, the troposphere is a non-dispersive medium. Thus, the tropospheric delay cannot be estimated from two-frequency measurements as can the ionospheric delay. Instead, estimation of the delay relies on the use of one of a number of models^[7]. The 'dry' component can be accurately estimated from models based on surface measurements of atmospheric pressure alone. The 'wet' component is more difficult to model, since measurements of meteorological conditions at the antenna site are generally not representative of conditions along the line of sight.

That several tropospheric models have been developed is mainly because of this difficulty in modelling the 'wet' component. Usually the delays are evaluated in the zenith direction. The zenith corrections are then 'mapped' down to lower angles of elevation using mapping functions. Models are either semi-empirical, based on surface measurements of the local temperature, atmospheric pressure and relative humidity, or empirical, based on a general reference atmosphere requiring only the station height and the angle of elevation to the satellite.

Of the semi-empirical models, some of the best known have been developed by Hopfield and Saastamoinen, and are widely used within the geodetic community. In this paper we use as reference a model developed by the Jet Propulsion Laboratory (JPL) for its deep space

missions^{18, 91}. Evaluated against balloon measurements, it was found that this model is able to predict the zenith tropospheric delays with an accuracy at the subnanosecond level.

The tropospheric corrections currently used by the timing community are computed according to general empirical models which neglect the contribution due to the 'wet' component. Consequently, the errors resulting from these simple models may exceed 3 ns in a one-way range delay at 20° angle of elevation. The three models usually implemented are NBS^[10], STI^[11] and STANAG^[12]. The STANAG model is recommended in recently established standards for GPS time receiver software. In previous papers these models have been compared with one another and with semi-empirical models. Differences can reach several nanoseconds for low elevation angles.

THE EXPERIMENT

To illustrate the possible impact on GPS common-view time transfer of the approximate models of tropospheric delay used in GPS time receivers, four time laboratories, listed below, were chosen. Several criteria contributed to this choice. The basic criterion was the availability of meteorological data recorded at the site. Next, two time laboratories had to be located in the same climatic zone (BIPM and OCA) and the other laboratories had to be situated as far away as possible and in climatic zones as different as possible. This last criterion was the most difficult to fulfil as can be seen from the table below, which lists the geographical latitudes of the sites.

Participating time laboratories in this experiment were:

BIPM, Bureau International des Poids et Mesures, Sèvres, France, Lat. = 49 N, H = 127 m,

OCA, Observatoire de la Côte d'Azur, Grasse, France, Lat. = 43 N, H = 1322 m,

USNO, United States Naval Observatory, Washington D.C., U.S.A., Lat. = 39 N, H = 51 m,

CRL, Communications Research Laboratory, Tokyo, Japan, Lat. = 36 N, H = 130 m.

The GPS time receivers operating at the BIPM, the OCA and the CRL used the NBS type tropospheric model, and the receiver used at the USNO used the STI type tropospheric model.

Four GPS common-view time links, listed below, were considered. The short baseline link, BIPM-OCA, was analysed to see if there is any impact of approximated tropospheric delay on GPS common-view time transfer in the same climatic zone. The three long baseline links were considered for their climatic differences and low angles tracks.

BIPM - OCA, of 700 km, with 32 daily CV possible, according to Inter. GPS CV Sched. No 20,
OCA - USNO, of 6400 km, with 18 daily CV possible, according to Inter. GPS CV Sched. No 20,
OCA - CRL, of 9000 km, with 14 daily CV possible, according to Inter. GPS CV Sched. No 21,
USNO - CRL, of 9600 km, with 8 daily CV possible, according to Inter. GPS CV Sched. No 21.

The BIPM-OCA link was analysed in terms of the available meteorological data for 22 and 23 April 1993, and three other links were analysed for 26 August 1993.

Elevation angles by track and location are given in Figures 1, 5, 9, and 13. For each link, the track was computed at both sites using both the simple empirical model in the receiver and the JPL semi-empirical model based on surface weather measurements. The results are given in Figures 2, 3, 6, 7, 10, 11, 14, and 15. Differences between the two models ranging from 0.4 ns to 1.1 ns for the short baseline link, and from 1 ns to 6 ns for long baseline links, can be observed. Next, the common views between the two sites were computed using the receiver and JPL models. The peak to peak differences between the two computations for individual common views do not exceed a few hundreds of picoseconds for the short baseline link (Figure 4) and reach 5 ns for the long distance links (Figures 8, 12, and 16). For two longest long links, OCA-CRL and OCA-USNO, a clear bias of a few nanoseconds may be observed. This is so because low elevation angles and limited number of common views were available. For the shortest of the long distance links, OCA-USNO, large discrepancies in the results may be seen (Figure 8). This is due to the large differences in the elevation angles at both sites (Figure 5).

CONCLUSIONS

1. The use of a standardized tropospheric model in GPS time receivers is essential for accurate time comparisons.
2. For GPS time links within a region of similar climate, the use of a simplified standard tropospheric model is sufficient for 1 nanosecond accuracy.
3. For intercontinental GPS time links: common views should be performed at the same elevations at each side, the use of a more sophisticated model based on surface measurements should be considered and studied more closely.

Acknowledgements

The experimental part of this work was done at the BIPM thanks to the loan of a commercial caesium clock from the USNO (Washington, DC, USA). The staff of the Time Section of the BIPM is grateful to the USNO for its generosity.

References

- [1] D. Kirchner, H. Bessler, and S. Fassi, "Experience with two collocated C/A code GPS receivers of different type," in Proc. 3rd European Time and Freq. Forum, pp. 94-103, March 1989.
- [2] W. Lewandowski and C. Thomas, "GPS Time Transfer," Proc. IEEE, vol. 79, pp. 991-1000, July 1991.

- [3] The Group on GPS Time Transfer Standards, "*Technical Directives for Standardization of GPS Time Receiver Software*," Rapport BIPM-93/6, 1993.
- [4] W. Lewandowski, G. Petit and C. Thomas, "*GPS Standardization for the needs of Time Transfer*," in Proc. 6th European Time and Freq. Forum, pp. 243-248, 1992.
- [5] D. Kirchner, C. Lentz and H. Ressler, "*Tropospheric Corrections to GPS Measurements Using Locally Measured Meteorological Parameters Compared with General Tropospheric Corrections*," in Proc. 25th PTTI, pp. 231-248, 1993.
- [6] W. Lewandowski, P. Grudler and F. Baumont, "*Study of Tropospheric Correction for GPS Common-View Time Transfer between the BIPM and the OCA*", in Proc. 8th European Time and Freq. Forum, Vol II, 1994.
- [7] G.M.R. Winkler, "*Path delay, its variations, and some implications for the field use of precise frequency standards*" Proc. IEEE, vol. 60, pp. 522-529, 1972.
- [8] G.A. Madrid, C.C. Chao, et al., "*Tracking System Analytic Calibration Activities for Mariner Mars 1971 Mission*," JPL Technical Report 32-1587, March 1, 1974.
- [9] H. F. Fliegel (The Aerospace Corporation, El Segundo, CA, USA), personal communication,
- [10] M. A. Weiss (NIST, Boulder, Co, USA), personal communication, 1989.
- [11] D. Kirchner (TUG, Graz, Austria), personal communication, 1991.
- [12] NATO Standardization Agreement (STANAG) 4294, Arinc Research Corporation, 2551 Riva Road, Annapolis, MD, 21401, USA, Publication 3659-01-01-4296, 1 August 1990.

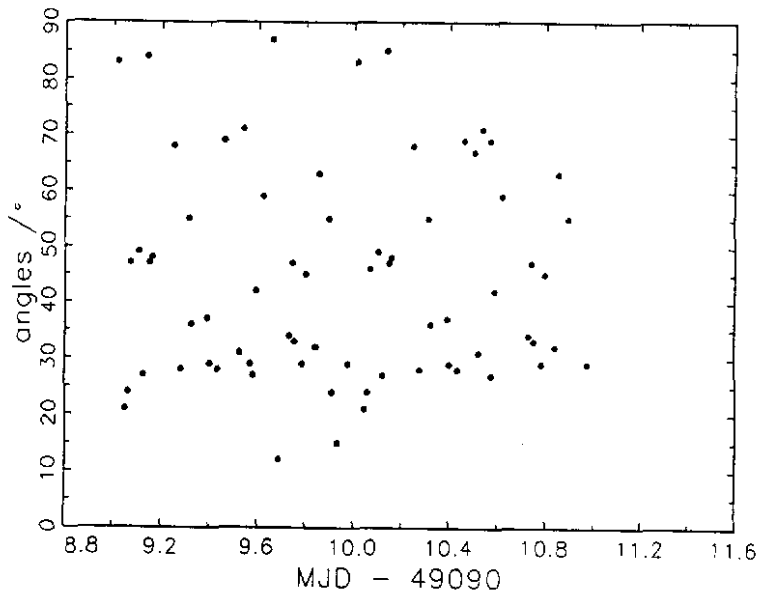


FIGURE 1. Elevation angles of each track on 22-23 April 1993 at the BIPM and OCA. They are the same within 1°.

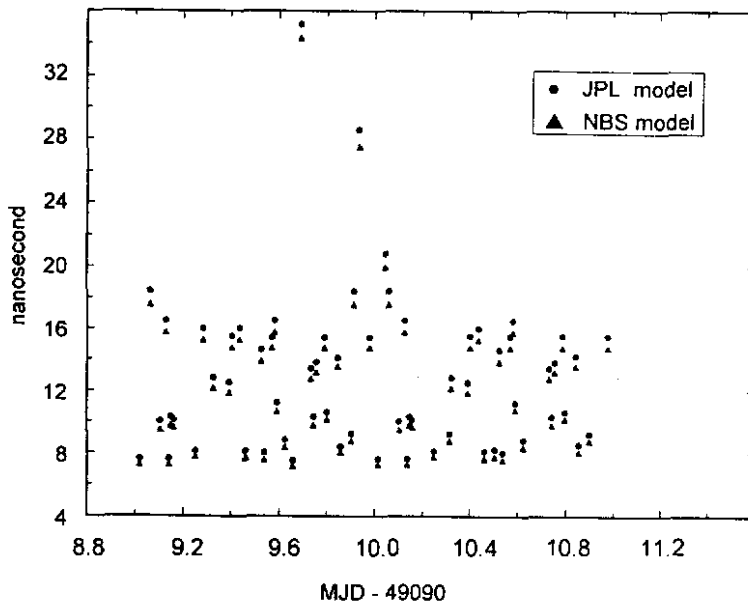


FIGURE 2. Tropospheric delays according to the JPL and the NBS models at the BIPM on 22-23 April 1993 for each track in the direction of the OCA.

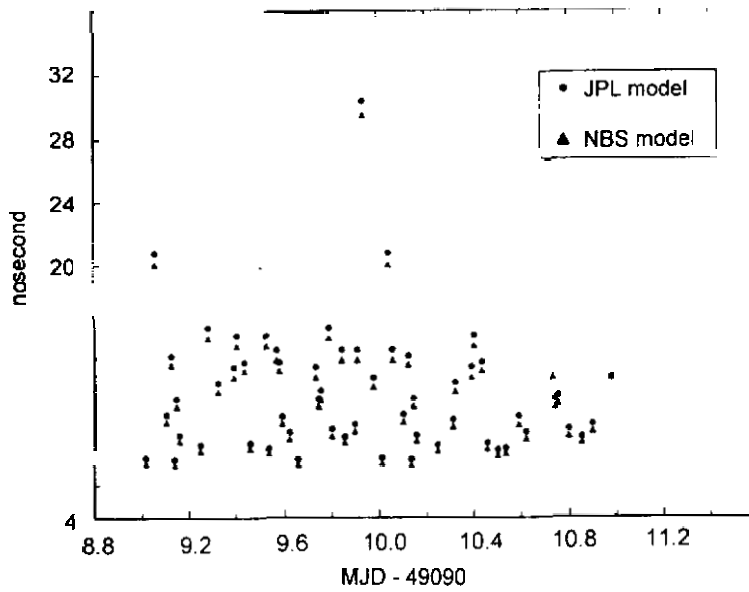


FIGURE 3. Tropospheric delays according to the JPL and the NBS models at the OCA on 22-23 April 1993 for each track in the direction of the BIPM.

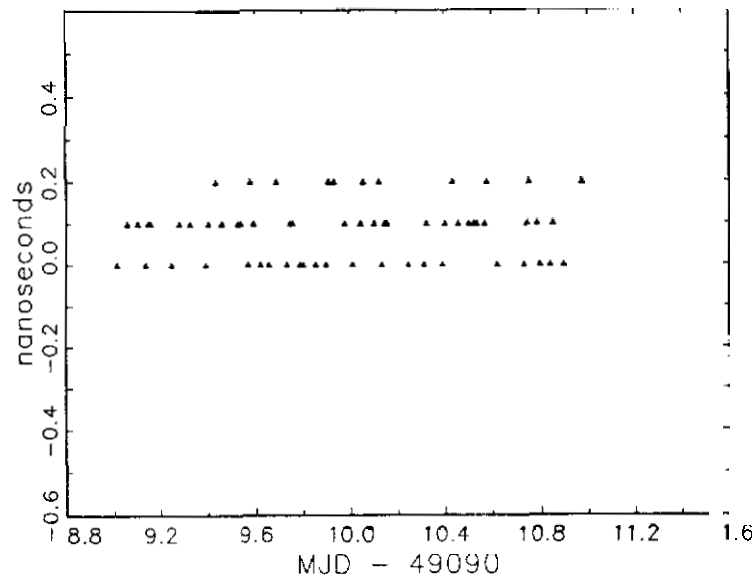


FIGURE 4. [BIPM Cs clock - OCA Cs clock] as obtained by GPS common views with the NBS tropospheric model minus [BIPM Cs clock - OCA Cs clock] as obtained by GPS common views with the JPL tropospheric model for each track on 22-23 April 1993.

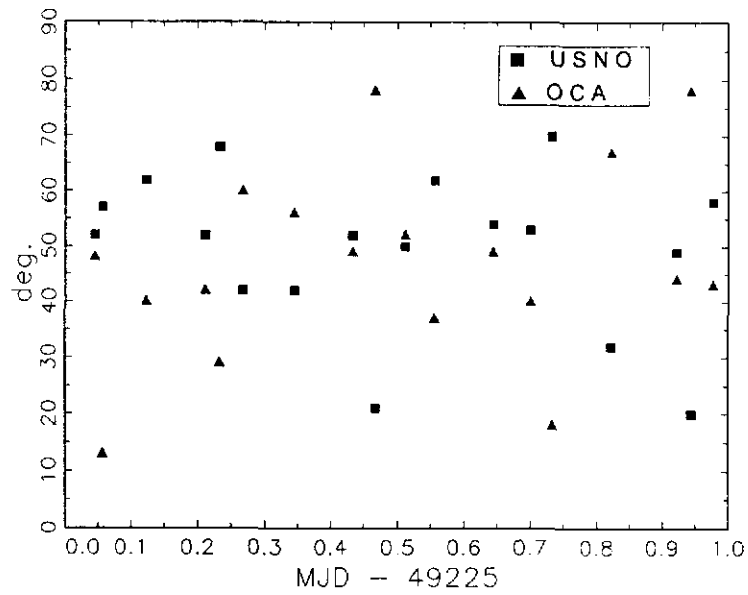


FIGURE 5. Elevation angles of each track on 26 August 1993 at the OCA in the direction of the USNO and at the USNO in the direction of the OCA.

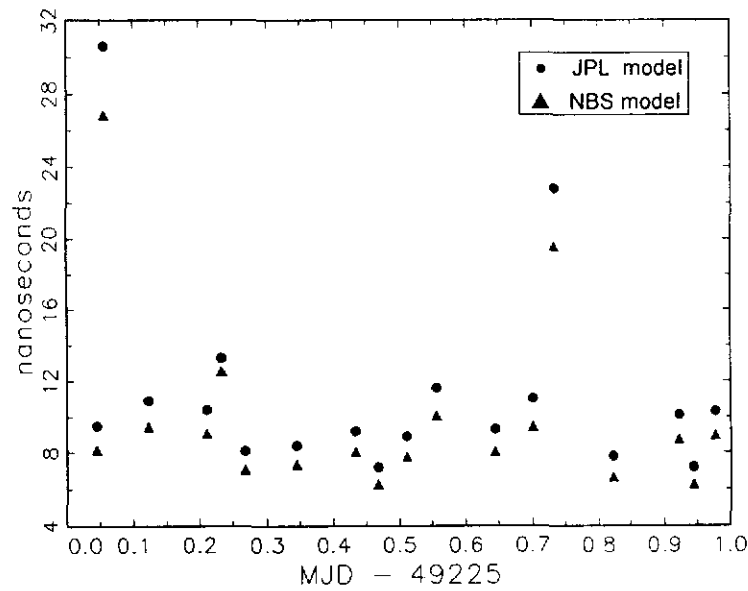


FIGURE 6. Tropospheric delays according to the JPL and the NBS models at the OCA on 26 August 1993 for each track in the direction of the USNO.

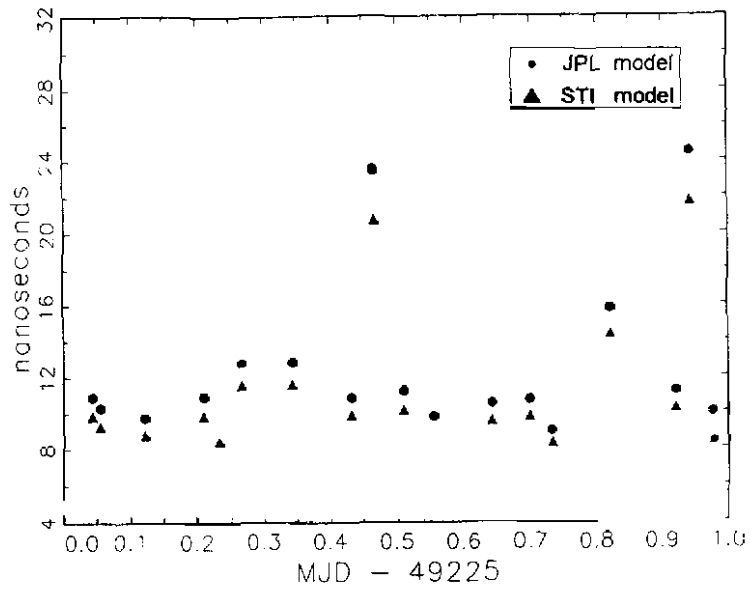


FIGURE 7. Tropospheric delays according to the JPL and the STI models at the USNO on 26 August 1993 for each track in the direction of the OCA.

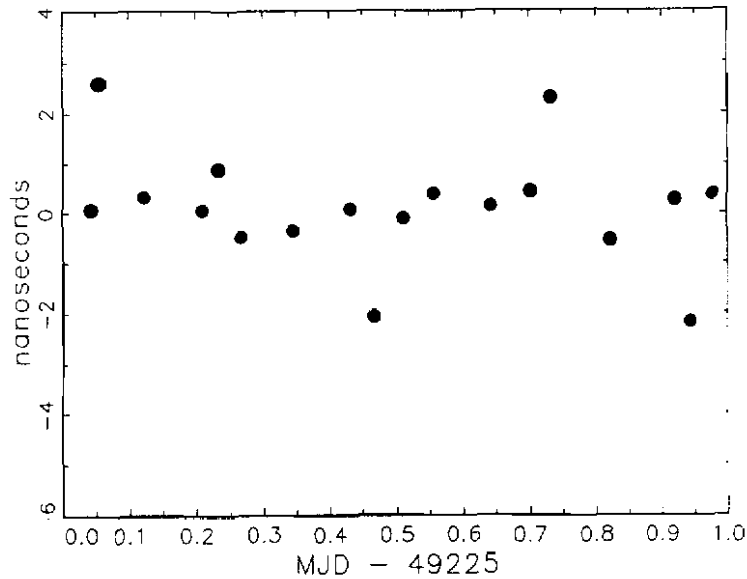


FIGURE 8. [OCA Cs clock - UTC(USNO Master Clock)] as obtained by GPS common views with the NBS and STI tropospheric models minus [OCA Cs clock - UTC(USNO Master Clock)] as obtained by GPS common views with the JPL tropospheric model for each track on 26 August 1993.

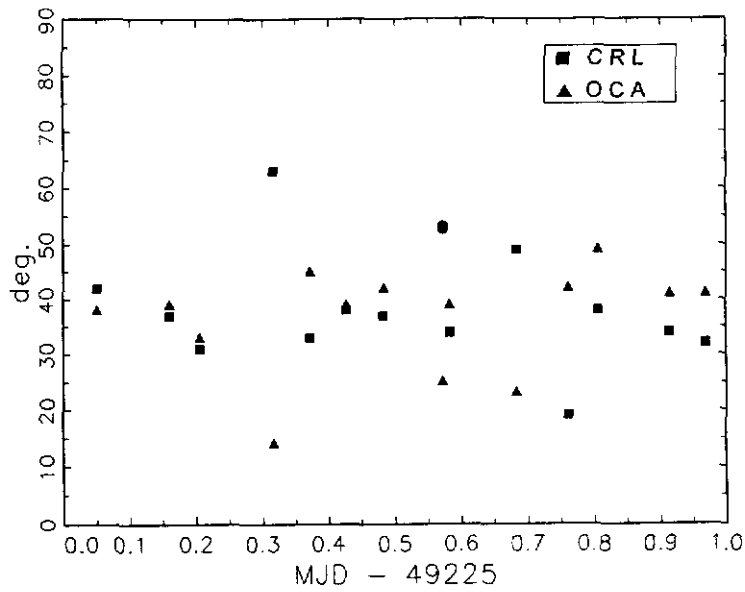


FIGURE 9. Elevation angles of each track on 26 August 1993 at the OCA in the direction of the CRL and at the CRL in the direction of the OCA.

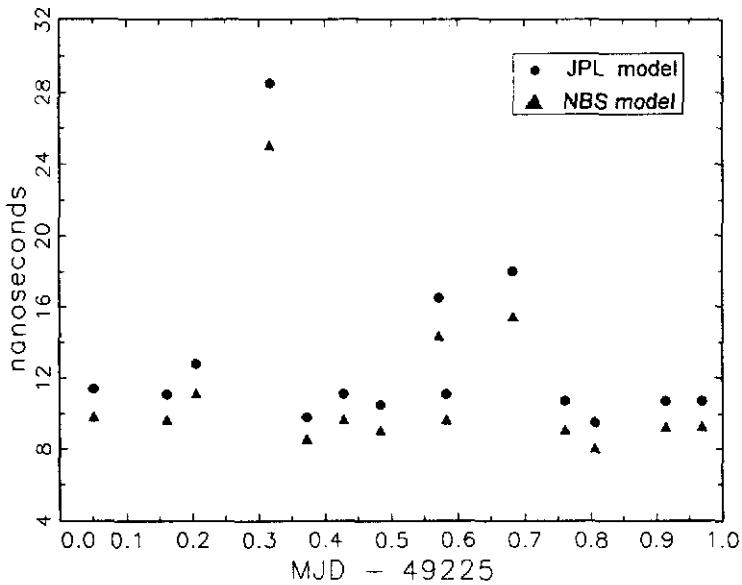


FIGURE 10. Tropospheric delays according to the JPL and the NBS models at the OCA on 26 August 1993 for each track in the direction of the CRL.

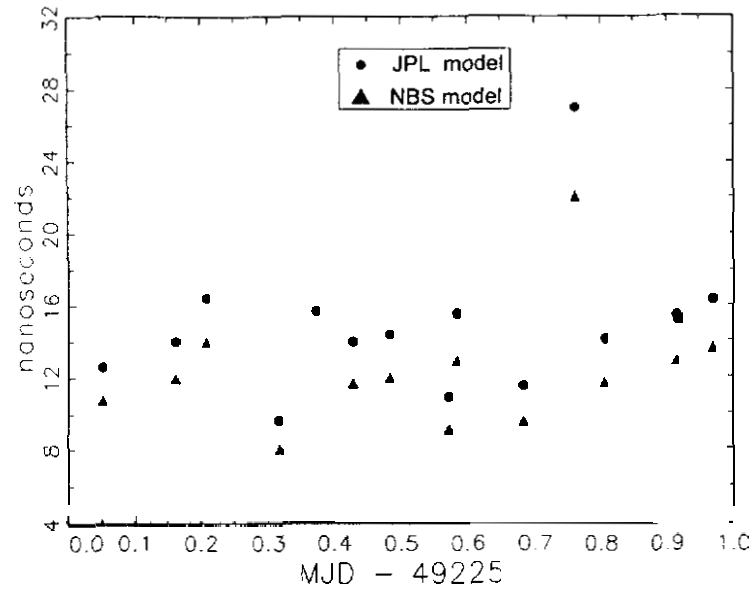


FIGURE 11. Tropospheric delays according to the JPL and the NBS models at the CRL on 26 August 1993 for each track in the direction of the OCA.

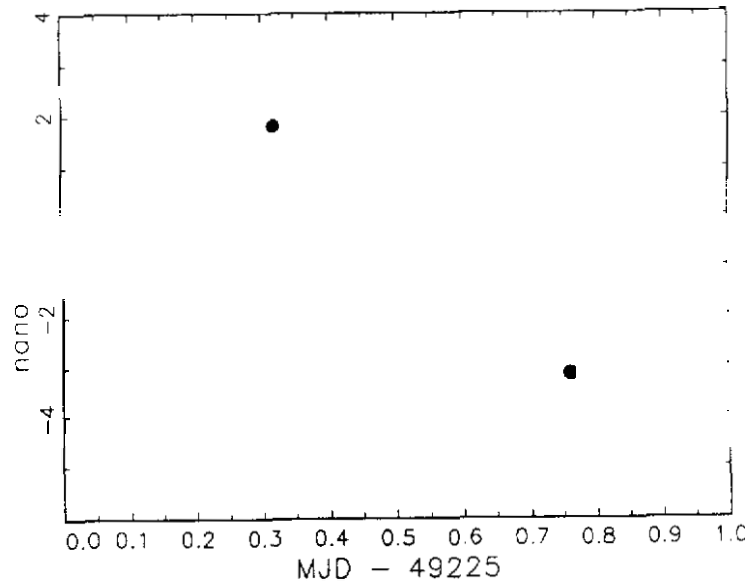


FIGURE 12. [OCA Cs clock - UTC(CRL)] as obtained by GPS common views with the NBS tropospheric model minus [OCA Cs clock - UTC(CRL)] as obtained by GPS common views with the JPL tropospheric model for each track on 26 August 1993.

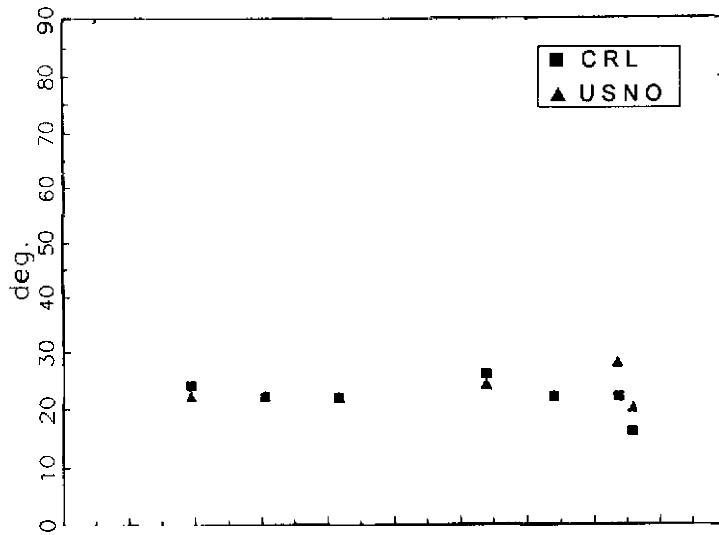


FIGURE 13. Elevation angles of each track on 26 August 1993 at the USNO in the direction of the CRL and at the CRL in the direction of the USNO.

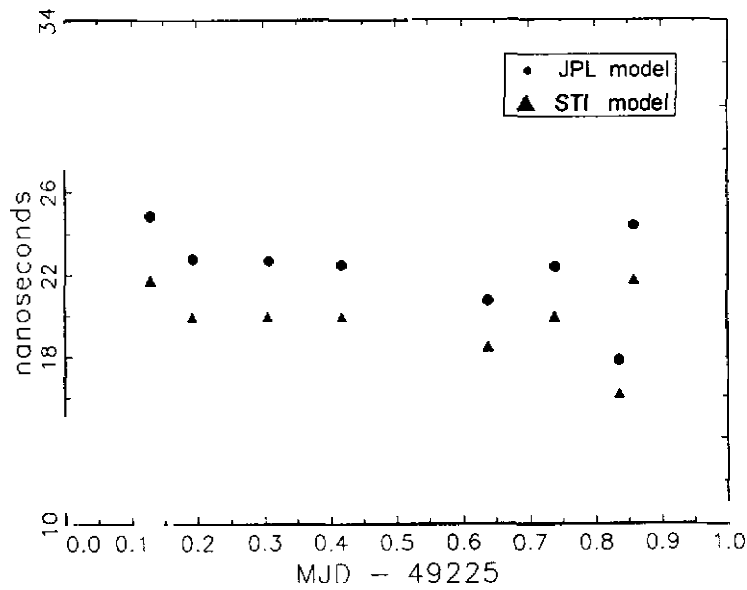


FIGURE 14. Tropospheric delays according to the JPL and the STI models at the USNO on 26 August 1993 for each track in the direction of the OCA.

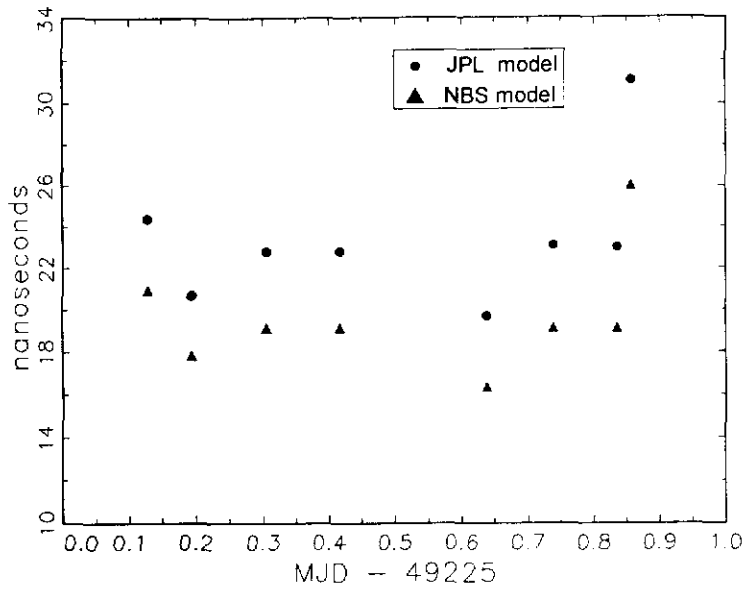


FIGURE 15. Tropospheric delays according to the JPL and the NBS models at the CRL on 26 August 1993 for each track in the direction of the USNO.

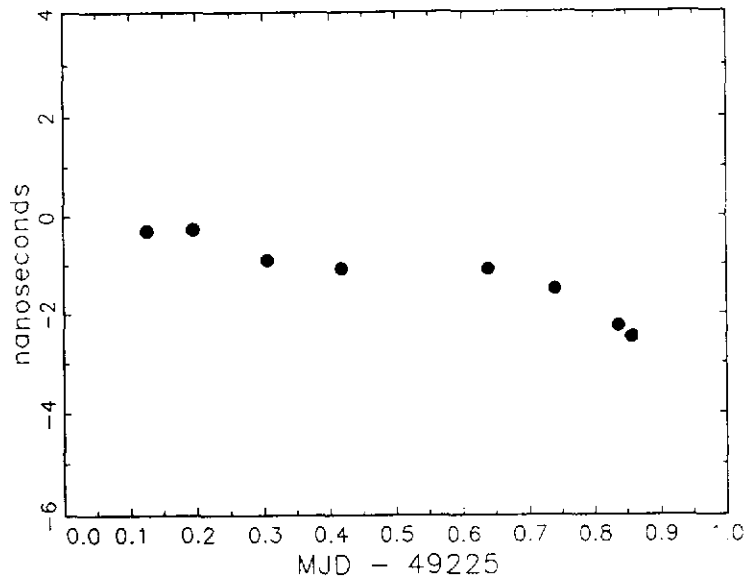


FIGURE 16. $[\text{UTC}(\text{USNO Master Clock}) - \text{UTC}(\text{CRL})]$ as obtained by GPS common views with the STI and NBS tropospheric model minus $[\text{UTC}(\text{USNO Master Clock}) - \text{UTC}(\text{CRL})]$ as obtained by GPS common views with the JPL tropospheric model for each track on 26 August 1993.

QUESTIONS AND ANSWERS

MARC WEISS (NIST): I wonder if you did a comparison of the effects of using measurements of humidity versus not using measurements of humidity, say, in the more accurate models, like the CHEL model? I'm asking this because even if we use the CHEL model, it's easy to use it in the receivers; but still, if we have to measure the humidity and have other measurements that go into it, that's a lot harder.

DR. LEWANDOWSKI (BIPM): It was considered to include in the standard format the measurement of humidity temperature. But this point was discussed, and finally the majority of the involved people decided not to do it, because of this external measurements to the receiver.

But there is a possibility to add additional columns with these measurements. But this issue of measuring meteor conditions comes in laboratories which measure international time links. So it's not of concern to many people; it's for those who want to do more accurate studies.

MARC A. WEISS (NIST): So my question is whether you compare using measurements versus not using measurements in the tropospheric model. What differences does that produce?

W. LEWANDOWSKI (BIPM): In measuring and not measuring? It was peak differences up to five ns in the intercontinental time links.

DAVID ALLAN (ALLAN'S TIME): I would like to actually make a comment in regard to the melting pot method which the USNO has introduced or has used, I think, quite effectively. In this case, of course, the satellites are at high elevation angles. And the question is -- and maybe this is really a question of Dr. Winkler -- one would like to do the same thing that has been done with common view, that is, go A to B, B to C, C back to A; and you get closure around the globe so you can test the around-the-world accuracy. And because of the high altitudes that you can achieve in using the melting pot method, it would be interesting to do the same thing, A to B, B to C, and go around the globe and check the closure on that. I don't know whether that's been done or not. Dr. Winkler, do you know?

W. LEWANDOWSKI (BIPM): Of course, using melting pot and high elevations improves the conditions. But again, for very accurate time links, measuring meteor conditions should be considered also, for any observations. If you want to go down under one ns.

At this moment, when we have troubles with receivers, they are noisy at the level of 10 ns, and this issue is not so urgent. But with future receivers, and if we want to go down under one ns, it should be gathered.